DOI: 10.1002/chem.200801552

Synthesis and Investigation of a Chiral Enterobactin Analogue Based on a Macrocyclic Peptide Scaffold

Áron Pintér and Gebhard Haberhauer*[a]

Abstract: A chiral C_3-symmetric enterobactin analogue (**1**) has been synthesized by attachment of three 2,3-dihydroxybenzoyl units to a chiral oxazole-containing macrocyclic peptide scaffold. Complex formation kinetics and stoichiometry with various metal ions were investigated by spectrophotometric methods. In the cases of Al^{III}, In^{III} and Fe^{III} complexes, UV absorption and CD kinetics showed nonlinearity, which results from slow conformational changes of the octahedral complexes. Virtual binding constants were determined from UV absorption data and showed selective binding of Ga^{III} in preference to Fe^{III}, by two orders of magnitude. CD spectroscopy revealed highly diastereoselective binding of Al^{III}, Ga^{III}, In^{III}, Fe^{III} and Ge^{IV} ions at room temperature, corresponding to the helical chirality opposite to that of the analogous enterobactin complexes. Ab initio calculations confirmed the energetic stabilization of the Λ isomers relative to the Δ isomers.

Keywords: amino acids · CD spectroscopy · enterobactin · macrocycles · oxazoles

Introduction

Enterobactin is a well-known triscatecholamide-type siderophore discovered almost 40 years ago. It is produced by *Escherichia coli* and related enteric bacteria in order to overcome iron-deficient conditions in living host organisms.[1] This low-molecular-weight iron(III) carrier is made up of three (*S*)-serine units that form a cyclic trilactone scaffold bearing three 2,3-dihydroxybenzamide binding arms.

Enterobactin possesses an extremely high affinity for Fe^{III} ions, and the proton-independent stability constant (β_{110}) of the $[Fe(ent)]^{3-}$ complex has been estimated to be $10^{49}\,M^{-1}$.[2] In addition, its octahedrally coordinated complexes of 1:1 stoichiometry with a variety of metal ions, such as Cr^{III},[3] Ga^{III},[4] Al^{III},[4a,5] In^{III},[4a,5] Sc^{III},[4a,5,6] Rh^{III},[7] and V^{IV}[8] have been described. The Fe^{II} complex of fully protonated enterobactin has also been verified.[9]

A matter of particular interest is the stereochemistry at the metal centres of the enterobactin metal complexes, as it is known that the configuration of the coordinated iron centre is crucial for the biological activity of the siderophore.[10] In enterobactin, the configuration at the C_3-symmetric metal centre is predetermined by the chiral cyclic trilactone scaffold, and the corresponding Δ-Fe^{III} complex is formed stereoselectively.[11] However, the calculated energy differences between the Λ and the Δ diastereomers of ferric enterobactin are low, varying between 2.1 and 8.6 $kJ\,mol^{-1}$ according to the level of theory,[12] which may be explained by the high flexibility of the trilactone platform.

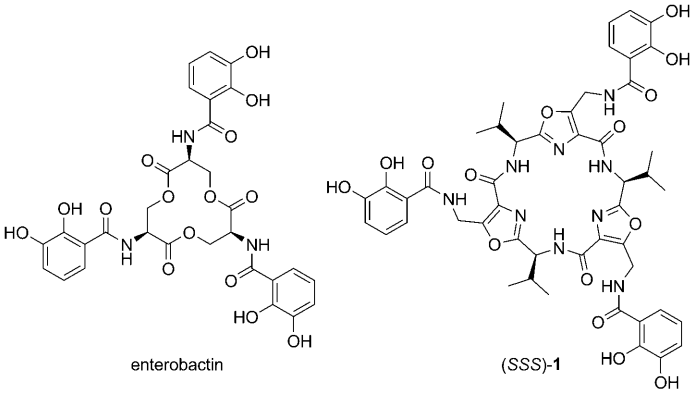

Although various enterobactin analogues based on C_3-symmetric oligo- or macrocyclic central units—such as 1,5,9-triaminocyclododecane,[13] 2,6,10-triaminotrioxatricornan,[14] cyclodextrin[15] or perhydrophenalene[16]—have been developed,[17] there are only a few examples of synthetic entero-

[a] Dr. Á. Pintér, Prof. Dr. G. Haberhauer
Institut für Organische Chemie, Fachbereich Chemie
Universität Duisburg-Essen, Universitätsstrasse 7
45117 Essen (Germany)
Fax: (+49)201 183 4252
E-mail: gebhard.haberhauer@uni-due.de

Supporting information for this article is available on the WWW under http://dx.doi.org/10.1002/chem.200801552.

bactin analogues that display diastereoselective metal complex formation.[18,19] In contrast with naturally occurring enterobactin, these analogues are each made up of three chiral binding arms attached to an achiral centre or achiral scaffold.

Our intention was to develop an enterobactin analogue consisting of a chiral scaffold and three achiral catecholate arms that would exhibit predictable and highly diastereoselective metal complex formation. As we had already used cyclic peptides containing imidazole and oxazole units in their backbones for the control of axial and planar chirality[20,21] and for chirality transfer in C_3-symmetric compounds,[22,23] we decided also to use this type of chiral scaffold for the design of a chiral synthetic enterobactin analogue. Here we report the synthesis of the triscatecholate ligand (*SSS*)-**1** and an extended study of the diastereoselective complex formation of **1** with various metal ions.

Results and Discussion

Synthesis of the ligand: The synthetic pathway for ligand **1** is depicted in Scheme 1. Firstly, methyl- and benzyl-protected acid chlorides **6a** and **6b** were synthesized by known procedures.[24] Deprotection of the tris(phthalimidomethyl)oxazole peptide scaffold **7**[23] by hydrazinolysis, followed by acylation with **6a** and **6b**, gave the corresponding protected ligands **8a** and **8b**, respectively. Deprotection of **8a** was accomplished by treatment with boron tribromide in dichloromethane, while **8b** was debenzylated by catalytic hydrogenolysis to afford the chiral triscatecholamide-type ligand **1**.

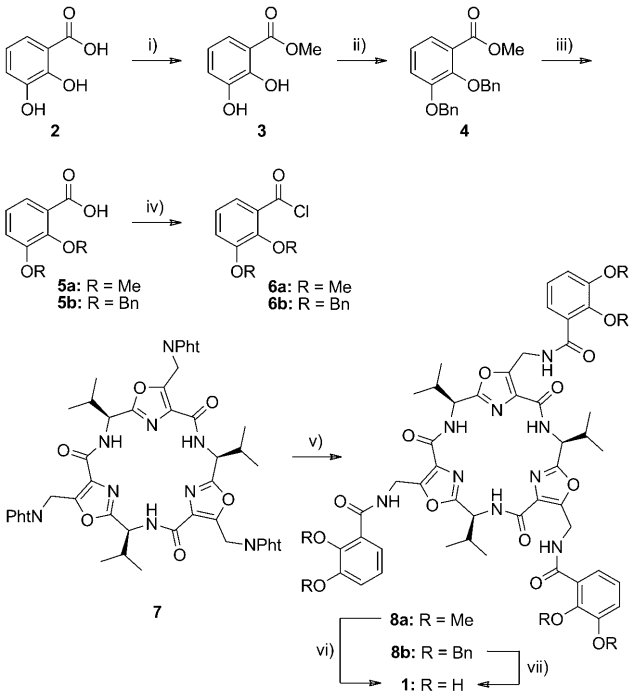

Scheme 1. Synthesis of ligand **1**: i) MeOH, $SOCl_2$, RT, 99%; ii) BnCl, K_2CO_3, DMF, 150°C, 97%; iii) NaOH, MeOH/H_2O, 100°C, then aq. HCl, 97%; iv) $SOCl_2$, Δ, 96% for **6a** and 99% for **6b**; v) 1) $N_2H_4{\cdot}H_2O$, THF/CH_2Cl_2/EtOH, RT; 2) **6a**/**6b**, CH_2Cl_2, Et_3N, RT, 99% for **8a** and 61% for **8b**. vi) BBr_3, CH_2Cl_2, RT then MeOH, 96%; vii) H_2/Pd(OH)$_2$/C, MeOH, 96%.

Analyses of the ligand **1**, as well as of the two precursors **8a** and **8b**, by ESI-MS, NMR and UV/Vis spectroscopy are in agreement with their structures. The ^{1}H NMR spectrum of **1** in [D$_4$]MeOH confirms an ideal C_3 symmetry with three catecholate binding arms rotating rapidly on the NMR timescale, as the diastereotopic protons of the amidomethyl groups show only a broad singlet at $\delta = 4.88$ ppm. In the cases of the ^{1}H NMR spectra of **8a** and **8b** in $CDCl_3$ the methylene signals are separated by 0.15 ppm as doublets of doublets. The spectrum of **8b** additionally reveals a small anisotropy of 0.03 ppm for the methylene protons of the *ortho*-benzyloxy protecting group. The methylene protons of the *meta*-benzyloxy group show only a singlet. The restricted rotation of the side arms is probably caused by intramolecular hydrogen bonds between the amide oxygens of the macrocyclic scaffold and the catecholamide protons, which explains their low-field chemical shifts ($\delta = 8.69$ ppm for **8a** and $\delta = 8.55$ ppm for **8b**). The hindered rotation of the *ortho*-benzyloxy group is a consequence of steric hindrance rather than intrastrand hydrogen bonding between ether oxygen and the neighbouring catecholamide proton.

Investigation of metal complex formation by HR-ESI mass spectroscopy: Complex formation by the triscatecholate ligand **1** with various trivalent and tetravalent metal ions at room temperature was first investigated by electrospray ionization mass spectroscopy. For this purpose, aqueous methanolic solutions (MeOH/H_2O 10:90) containing the ligand **1** and the appropriate metal salt in equal concentrations (5.0×10^{-5} M) together with NaOH (10^{-2} M) were prepared and measured with negative and positive ion detection. In both modes the measured mass spectra show signals of highest intensity for the doubly charged ions $[L^{6-}+M^{n+}+(4-n)H^+]^{2-}$ and $[L^{6-}+M^{n+}+(8-n)Na^+]^{2+}$, respectively. Whereas for the ions Al^{III}, Ga^{III}, In^{III}, Fe^{III}, Sc^{III}, Y^{III}, Ti^{IV} and Ge^{IV} the peaks of the corresponding metal complexes were found, for the other metal complexes no signals could be detected (Table 1 and Table 2). Interestingly, the exact masses of the dianion peaks obtained for the In^{III} and Sc^{III} complexes do not correspond to the single protonated metal complexes but to the fully deprotonated ligand with the metal cation lacking one negative charge. This may be attributed to the formation of radical anions under the conditions of negative ionization.

Investigation of complex formation by UV/Vis absorption and CD spectroscopy: In a first step, the kinetics of the metal ion binding were investigated by mixing the ligand **1** and the metal solutions in a molar ratio of 1:1.5 and simultaneous measuring UV absorption and CD spectra as a function of time. For the Al^{III}, In^{III} and Fe^{III} ions, relatively slow complex formation was found (Figure 1). To attain 95% of the final UV absorption change (at 270 nm), 4 minutes

Table 1. Calculated and experimentally measured exact masses of the complexes of **1** with trivalent metal ions recorded in the negative ion mode.

Metal ion	Formula	Calcd mass	Exptl mass
Al^{3+}	$[C_{48}H_{46}N_9O_{15}+Al]^{2-}$	507.6470	507.6451
Ga^{3+}	$[C_{48}H_{46}N_9O_{15}+Ga]^{2-}$	528.6190	528.6145
In^{3+}	$[C_{48}H_{45}N_9O_{15}+In]^{2-}$	551.1043	551.1034
Fe^{3+}	$[C_{48}H_{46}N_9O_{15}+Fe]^{2-}$	522.1237	522.1254
Ru^{3+}	$[C_{48}H_{46}N_9O_{15}+Ru]^{2-}$	545.1079	–
Rh^{3+}	$[C_{48}H_{46}N_9O_{15}+Rh]^{2-}$	545.6084	–
Cr^{3+}	$[C_{48}H_{46}N_9O_{15}+Cr]^{2-}$	520.1259	–
Sc^{3+}	$[C_{48}H_{45}N_9O_{15}+Sc]^{2-}$	516.1303	516.1269
Y^{3+}	$[C_{48}H_{46}N_9O_{15}+Y]^{2-}$	538.6091	538.6026
La^{3+}	$[C_{48}H_{46}N_9O_{15}+La]^{2-}$	563.6089	–

Table 2. Calculated and experimentally measured exact masses of the complexes of **1** with tetravalent metal ions recorded in the negative ion mode.

Metal ion	Formula	Calcd mass	Exptl mass
Ti^{4+}	$[C_{48}H_{45}N_9O_{15}+Ti]^{2-}$	517.6266	517.6244
Zr^{4+}	$[C_{48}H_{45}N_9O_{15}+Zr]^{2-}$	538.6047	538.6024
Ge^{4+}	$[C_{48}H_{45}N_9O_{15}+Ge]^{2-}$	530.6135	530.6111
Sn^{4+}	$[C_{48}H_{45}N_9O_{15}+Sn]^{2-}$	553.6040	–

under the given conditions (MeOH/H_2O 10:90, 0.10 M tris, 0.02 M HCl, pH 8.95, 20 °C) were required for Al^{III}, 30 minutes for Fe^{III} and 40 minutes for In^{III}.

However, the shapes of the corresponding CD kinetic curves differ significantly. In the case of Al^{III} the same cut-off value of the ellipticity change (at 265 nm) is obtained after about 32 minutes, while the Fe^{III} and In^{III} complexes require more than 60 minutes to obtain equilibrium. The incongruity of the normalized UV absorption and CD kinetic curves indicates continuous conformational changes of the formed complexes after coordination of the metal centre until the adoption of the final equilibrium conformation. In the cases of Ga^{III}, Ge^{IV} and Ti^{IV} ions, both complexation and adoption of the equilibrium conformation occur within a few seconds, and accordingly no time dependency—neither for the extinction nor for the ellipticity values—could be observed.

For the determination of thermodynamic parameters of the metal complexes of **1**, discontinuous titration experiments were performed with an automated titration unit connected to the spectropolarimeter. In the cases of Ru^{III}, Rh^{III}, Cr^{III}, Sc^{III}, Y^{III}, La^{III}, Zr^{IV} and Sn^{IV}, titration of **1** failed to produce any detectable spectral changes, indicating that there is no complex formation at constant basic pH value. In contrast, the electronic spectrum of **1** showed gradual changes if Al^{III}, Ga^{III}, In^{III}, Fe^{III}, Ge^{IV} or Ti^{IV} ions were used as guests. The UV spectrum of **1** shows three main absorptions, located at wavelengths around 220, 250 and 325 nm. The oxazole scaffold and catecholamide side arms contribute to the absorption at the shortest wavelength, whereas the other transitions can only be attributed to the newly formed chromophore. If titration was conducted with Ga^{III} ions, all absorption bands showed a moderate bathochromic

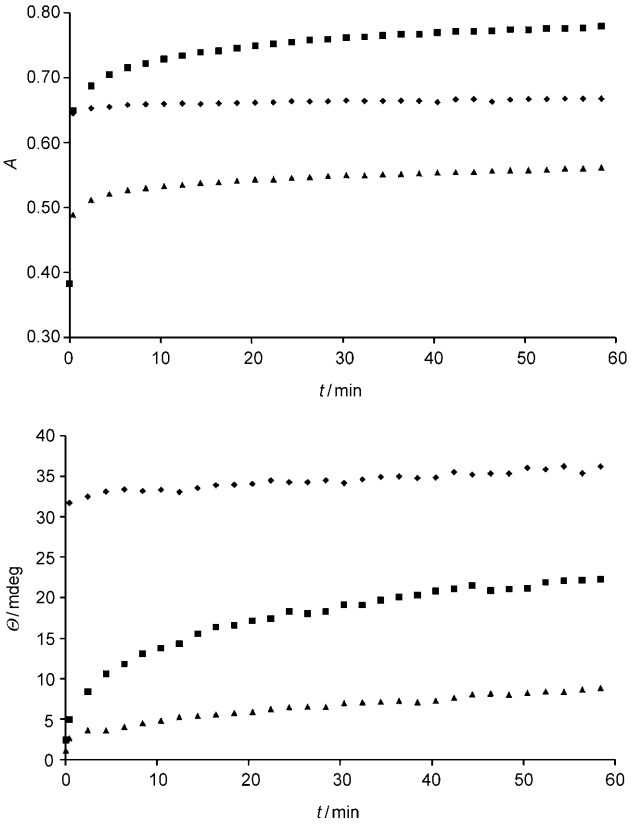

Figure 1. Complex formation kinetics of **1** with different metals (◆: Al^{III}, ■: Fe^{III}, ▲: In^{III}) ([**1**] = 2.4×10^{-5} M, [M]/[L] = 1.5, MeOH/H_2O 10:90; 0.10 M tris; 0.02 M HCl buffer, pH 8.95). Top) UV absorption measured at 270 nm. Bottom) Ellipticity measured at 265 nm.

shift, while changes in the CD spectrum were more striking (Figure 2). With increasing metal/ligand ratio, two strong positive Cotton effects emerge at 267 and 244 nm, accompanied by a small negative one at 322 nm, which could not be found in the spectrum of the uncomplexed ligand. The strong positive bands represent an exciton coupling due to the proximity of the helically coordinated catecholate arms around the metal centre, whereas the sign of their ellipticities implies a left-handed (Λ) orientation as the preferred conformation.[19b]

The UV spectral changes at different wavelengths upon addition of Ga^{III} to **1** are shown in Figure 3. The same spectral changes in the UV region could also be observed during the titration of **1** with Al^{III}, Fe^{III} and In^{III}, although longer mixing times of up to 15 minutes were required after each incremental addition of the titrant.

In the case of Ge^{IV}, only one narrow and strong positive Cotton effect arose between 250 and 280 nm as a result of complexation, and the final bathochromic shift of the absorption signals was the smallest among the observed complexes. If titration of ligand **1** was performed with Ti^{IV}, a significant bathochromic shift of all absorption bands and a yellow colouration could be observed, but the CD spectra showed no characteristic exciton coupling bands for octahedral complex formation. These observations may be ex-

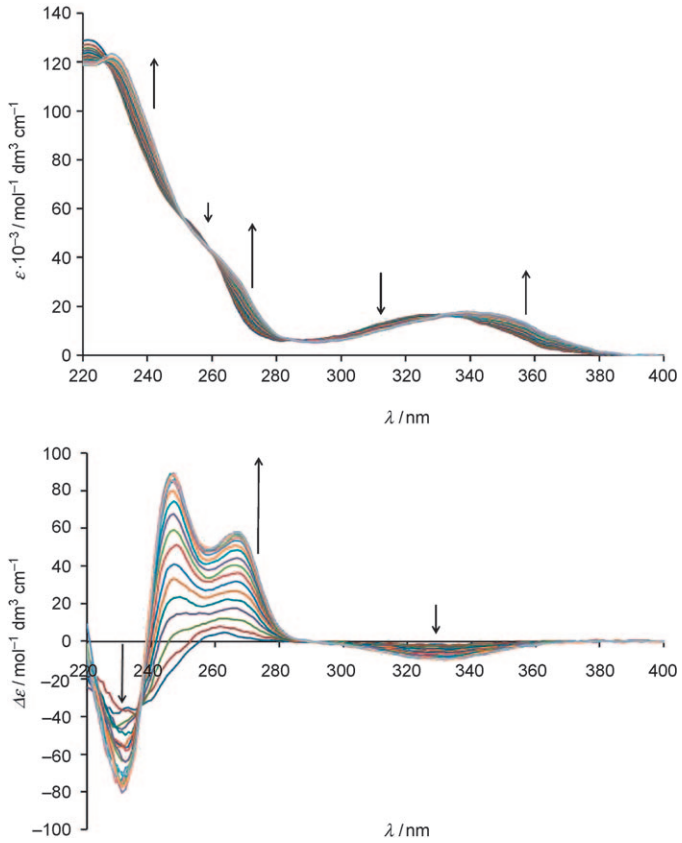

Figure 2. Spectrophotometric titration of ligand **1** with Ga^{3+} ([**1**] = 2.0×10^{-5} M, MeOH/H_2O 10:90; 0.10 M tris; 0.02 M HCl buffer; pH 8.95). Top) UV absorption spectra. Bottom) CD spectra.

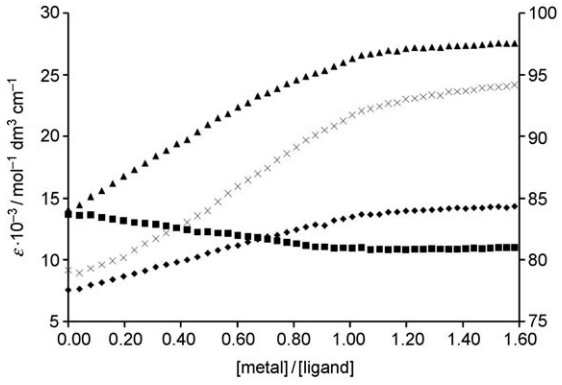

Figure 3. UV absorption titration curves (◆: 355, ■: 315, ▲: 270, ×: 240 nm) for complexation of **1** and Ga^{3+} at different wavelengths ([**1**] = 2.0×10^{-5} M, MeOH/H_2O 10:90; 0.10 M tris; 0.02 M HCl buffer; pH 8.95).

Table 3. CD spectra of the complexes of ligand **1** with metal ions M^{n+} ([**1**] = 2.0×10^{-5} M and **1**/M^{n+} = 1:1) in MeOH/H_2O (10:90; 0.10 M tris, 0.02 M HCl) at pH 8.95.

M^{n+}	$\Delta\varepsilon$ [mol^{-1} cm^{-1}] (λ [nm])			
–	−42.7 (234)	–	+4.8 (263)	
Al^{3+}	−66.6 (231)	+86.7 (247)	+56.0 (266)	−9.5 (330)
Ga^{3+}	−74.9 (232)	+82.7 (247)	+52.7 (267)	−9.2 (328)
In^{3+}	−45.2 (232)	–	+12.7 (264)	−2.5 (328)
Fe^{3+}	−43.6 (233)	–	+15.9 (265)	−3.9 (329)
Ge^{4+}	−19.3 (232)	–	+63.3 (262)	−7.0 (323)

photoactive species predominate in each solution. Additional Job plot analyses of the two-component systems of **1** with Al^{III}, Ga^{III}, Fe^{III} and Ge^{IV} gave evidence of pure 1:1 stoichiometry (Figure 4).

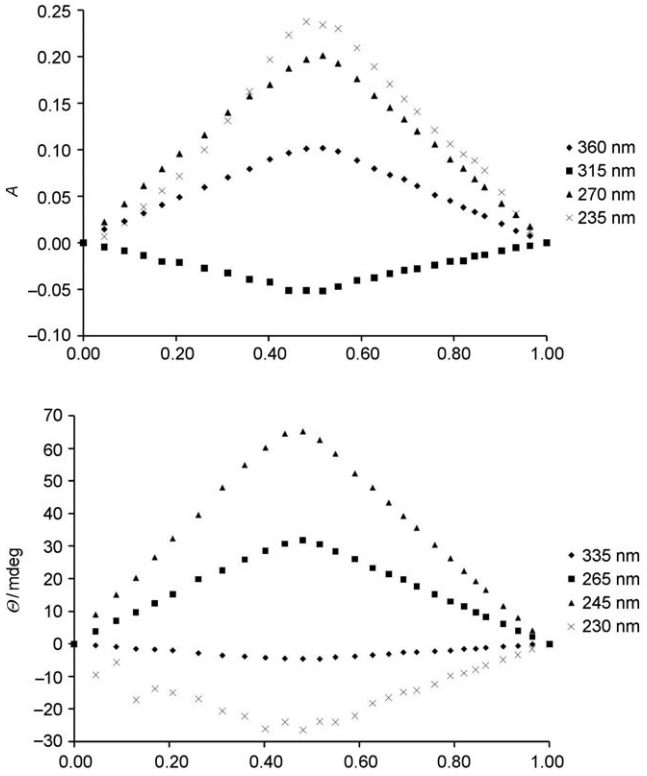

Figure 4. UV absorption and CD Job plots for complexation of **1** with Ga^{3+} at different wavelengths ([**1**]+[$GaCl_3$] = 3.0×10^{-5} M, MeOH/H_2O 10:90, 0.10 M tris/0.02 M HCl buffer, pH 8.95). Top) {$y = A_{obs.} - A_L - (A_M - A_L)\times x$ versus $x = [GaCl_3]/([GaCl_3]+[\mathbf{1}])$}. Bottom) {$y = \theta_{obs.} - \theta_L - (\theta_M - \theta_L)\times x$ versus $x = [GaCl_3]/([GaCl_3]+[\mathbf{1}])$}.

plained in terms of a low stability of the Ti^{IV} octahedral complex and the formation of yellow polymeric Ti^{IV}/catecholate compounds.[25] CD spectral data obtained for the triscatecholate ligand **1** and for its metal complexes are summarized in Table 3.

With the exception of titration with Ti^{IV} ions, UV and CD spectra each showed one set of isosbestic points during the whole process of titration, which indicates that only two

The affinities of ligand **1** for the metals under the conditions employed were evaluated as virtual binding constants according to Equation (1), which represents a simplified association constant involving all protonation/deprotonation and metal ion coordination steps. Although this constant is only applicable for the pH value applied for the measurement, it can provide information about the selectivity toward different cationic guests.

$$K_{LM}^{virt} = \frac{[LM]}{([L]_{tot}-[LM])([M]_{tot}-[LM])} \quad (1)$$

The virtual association constants of the complexation systems were calculated by nonlinear least-squares fitting according to the modified Benesi–Hildebrand equation from both UV absorption and CD data set.[26] The best reproducible results and the smallest errors could be obtained if absorption values between 265 and 275 nm or ellipticity values in the range of the exciton coupling band were used for evaluation. The obtained binding constants and free energy changes of **1** with cations are summarized in Table 4.

Table 4. Virtual binding constants (K_a) and overall free energy of complexation ($-\Delta G°$) between **1** and cations as determined by UV titration experiments (MeOH/H_2O 10:90; 0.10 M tris; 0.02 M HCl buffer; pH 8.95, 20 °C).

M^{n+}	K_a [$dm^3 mol^{-1}$]	$-\Delta G°$ [$kJ mol^{-1}$]	R^2
Al^{3+}	$(2.64\pm0.28)\times10^{6}$[a]	36.0	0.99935
Ga^{3+}	$(1.45\pm0.46)\times10^{6}$[a]	34.6	0.99651
In^{3+}	$(1.10\pm0.10)\times10^{4}$[b]	22.7	0.99608
Fe^{3+}	$(2.45\pm0.08)\times10^{4}$[c]	24.6	0.99944
Ge^{4+}	$(2.50\pm0.26)\times10^{6}$[d]	35.9	0.99937

Association constants were determined: [a] at 270 nm. [b] At 273–266 nm. [c] At 274–267 nm from UV absorption data set. [d] At 265–258 nm from CD data set.

The relative order of stability of the trivalent metal complexes with the macrocyclic ligand **1** is $Al^{3+} > Ga^{3+} > Fe^{3+} > In^{3+}$, suggesting that the maximum stability is achieved with the smallest cation. However, it is unlikely that the observed trend in complex stability constants for the metal ions can be entirely attributed to the size of the metal cation radii, since the ionic radii of Ga^{III} and Fe^{III} (62 and 64.5 pm)[27] are quite similar.

In order to provide more exact information about the sense of chirality at the metal centre in the complexes of **1**, absorption and CD spectra of the iron(III) complex in the visible region were investigated (Figure 5). Upon coordination of Fe^{3+} ions a red-coloured complex is formed from **1** in basic solution. The broad absorption band at 509 nm (ε = 5905 $mol^{-1} dm^3 cm^{-1}$) is assigned to a ligand-to-metal charge transfer (LMCT) band, which is characteristic for iron(III) octahedrally coordinated by three catecholate units. The corresponding CD spectrum shows a positive Cotton effect at longer wavelengths and a negative Cotton effect at shorter wavelengths relative to the LMCT band. Comparison with CD spectra of Cr^{III}[3] and Fe^{III}[28] enterobactin complexes clearly indicates that octahedral metal complexes of ligand **1** occur as stereoisomers with helicity opposite to that observed with naturally occurring enterobactin: namely Λ-*fac*.

The extent of diastereoselective complex formation caused by the chiral macrocyclic scaffold of ligand **1** was further investigated by ab initio calculations.[29] Full geometry optimizations were performed for the (*SSS*,Δ)- and (*SSS*,Λ)-complexes of **1** and for the Δ- and Λ-complexes of enterobactin by the DFT method (for a schematic representation of the two possible conformers of the metal triscatecholate complexes of **1** see Figure 6). In the case of the In^{III} complexes the structures were calculated at the B3LYP/Lan2LDZ level of theory; for all other complexes the B3LYP/6-31G* approximation was used (Table 5). The energy differences between the diastereomers of **1** vary between 51 and 55 $kJ mol^{-1}$ in favour of the (*SSS*,Λ)-stereoisomers, which accounts for a complete diastereoselectivity at room temperature according to the Boltzmann–Gibbs distribution. Interestingly, these energy differences are four to six times larger than the values calculated for the corresponding

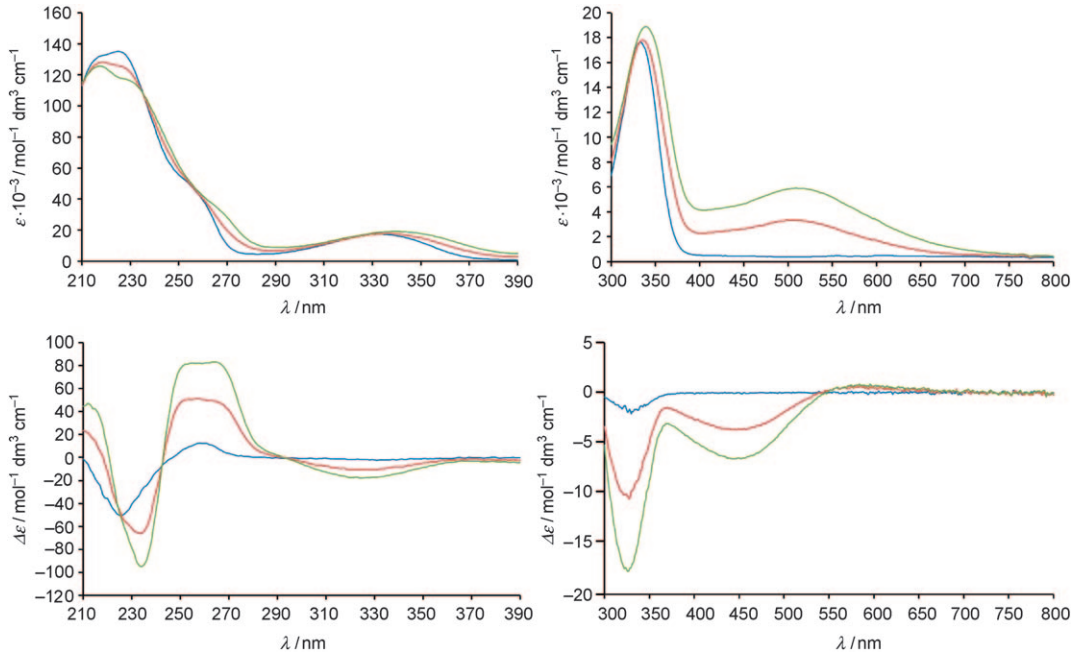

Figure 5. UV/Vis and CD spectra of **1** with 0.0 (——), 0.5 (——) and 1.0 (——) equivalents of Fe^{III} ([**1**] = 1.25×10^{-4} M in MeOH/H_2O 80:20; 0.10 M tris buffer).

Table 5. Relative energies of the conformers of **1**·$M^{(6-n)-}$ and enterobactin·$M^{(6-n)-}$ calculated (B3LYP) in kJ mol^{-1}.

Basis set	Isomer	Al^{III}	Ga^{III}	In^{III}	Ti^{IV}	Ge^{IV}
6-31G*	(*SSS*,Λ)-**1**	0.0	0.0		0.0	0.0
	(*SSS*,Δ)-**1**	52.4	54.9		53.1	50.9
	Λ-enterobactin	9.2	7.9		9.6	12.6
	Δ-enterobactin	0.0	0.0		0.0	0.0
Lan2DZ	(*SSS*,Λ)-**1**			0.0		
	(*SSS*,Δ)-**1**			55.4		
	Λ-enterobactin			8.4		
	Δ-enterobactin			0.0		

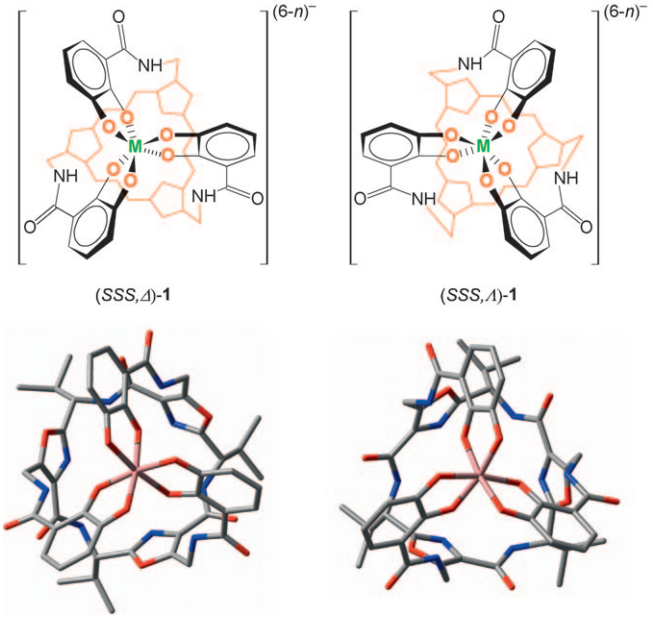

Figure 6. Top) Schematic representation of the two possible conformers of the triscatecholate complexes of **1**. Bottom) Molecular structures of the diastereomers of the complex **1**·Ga^{3-} calculated at the B3LYP/6-31G* level of theory; all hydrogen atoms have been omitted for clarity.

enterobactin complexes. On the assumption that the enthalpy of hydrolysis does not differ significantly for the two possible helical isomers, this stereoselectivity must persist in solution, too. This is in accordance with the results obtained by the CD measurements.

The optimized structures of the energetically favoured (*SSS*,Λ)-configured complexes of **1** show distorted octahedral geometries, in which twist angles (60° for perfect octahedral geometry) vary between 44 and 54°. In addition, the calculated M–O^{meta} bond lengths are 0.04–0.10 Å shorter than those of the M–O^{ortho} bonds. This may be due to the considerable diameter of the cyclohexapeptide platform, which is oversized in comparison with the only 12-membered and conformationally more flexible macrocyclic frame of enterobactin. To minimize constraints in the octahedral coordination sphere, complex formation is accompanied by considerable changes in platform conformation in relation to the structures of oxazole cyclohexapeptides without coordinatively or covalently anchored side arms. While platforms **7**, **8a** and **8b** exist in conformations with slight deviations of the oxazole rings from the reference planes, the 18-membered backbones of the modelled complexes of **1** adopt deeper, bowl-like conformations, through turning of the oxazole units inward when viewed from the direction of the metal centre. The identical vicinal $^3J_{HN,CH}$ values of 7.8–7.9 Hz for the protected ligands **8a** and **8b** and for the protected platform **7** correspond to dihedral angles of $145 < \Theta < 150°$,[30] which are in good agreement with the calculated and X-ray structures of the unsubstituted C_3-symmetric oxazole analogue from a previous study.[31] In these systems the dihedral angles χ [N_{amide}-C_α-$C_{oxazole}$-$O_{oxazole}$] can be taken to express the extent of deviation from planarity. In the case of complete planarity, this angle is 180°. While the optimized structures of unsubstituted oxazole cyclohexapeptides display cone angles of 160–169°, values of only 115–117° for the (*SSS*,Λ) isomers and 122–123° for the (*SSS*,Δ) isomers were obtained for the calculated complexes of **1**. Consequently, the preference for the Λ isomer in metal complexes of **1** cannot be a result of conformational constraints that exist within the 18-membered macrocycle. The reason for the large energy gap between the isomers is probably the distance between the carbonyl groups of the side chains and the carbonyl groups of the macrocyclic scaffold. In the case of the Λ isomers, the distance between the oxygen atoms of these groups are almost 6 Å, whereas in the case of the Δ isomers it is calculated to be 3.48–3.78 Å. This short distance causes repulsive interactions between the side arms and the scaffold, thus explaining the high energetic discrimination between the isomers.

Conclusion

In summary, we have been able to show that a C_3-symmetric oxazole-containing macrocyclic peptidic scaffold can be used for the construction of a siderophore ligand. Like the naturally occurring enterobactin, this siderophore consists of three achiral catecholate arms attached to a chiral backbone and forms octahedral metal complexes with high diastereoselectivity. Although iron(III) and gallium(III) have similar charge/radius ratios and normally produce similar octahedral complexes, the behaviour of the siderophore analogue towards these ions is different. While iron(III) ions are bonded slowly, the incorporation of Ga^{III} proceeds within seconds and the corresponding binding constant is higher by two orders of magnitude. The often used postulation that the group 13 metal ion gallium(III) can serve as an excellent surrogate marker of the iron(III) failed in this case.

Experimental Section

General remarks: All chemicals were reagent grade and were used as purchased. Reactions were monitored by TLC analysis with silica gel 60 F_{254} thin-layer plates. Flash chromatography was carried out on silica gel 60 (230–400 mesh). ^{1}H and ^{13}C NMR spectra were measured with Bruker Avance DMX 300 and Avance DRX 500 spectrometers. All chemical shifts (δ) are given in ppm relative to TMS. The spectra were

referenced to deuterated solvents indicated in brackets in the analytical data. HRMS spectra were recorded with a Bruker BioTOF III Instrument. IR spectra were measured on a Varian 3100 FT-IR Excalibur Series spectrometer. UV/Vis absorption spectra were obtained with a Varian Cary 300 Bio instrument, whereas CD absorption spectra were taken with a Jasco J-815 spectrophotometer fitted with a Jasco ATS-443 automatic titration unit.

Abbreviations: PhtN: phthalimido. THF: tetrahydrofuran. Tris: tris(hydroxymethyl)aminomethane.

Methyl 2,3-bis(benzyloxy)benzoate (4): A mixture of methyl ester **3** (1.345 g, 8.0 mmol), K_2CO_3 (3.428 g, 24.8 mmol), benzyl chloride (2.431 g, 19.2 mmol) and DMF (10 mL) was stirred at 150 °C for 60 minutes. After completion of the reaction, the mixture was cooled down, water (100 mL) was added, and the product was extracted with CH_2Cl_2 (3× 50 mL). The organic layer was dried over $MgSO_4$, filtered and evaporated to give an oily product, which was further exhaustively dried in vacuo (<1 mbar, 60 °C) to yield **4** (2.704 g, 97.0 %) as a clear yellowish oil. ^{1}H NMR (300 MHz, $CDCl_3$): δ = 7.47–7.41 (m, 4H; BnO ***CH***), 7.39–7.31 (m, 7H; BnO ***CH*** and Ph ***CH***-6), 7.16 (dd, $^3J_{H,H}$ = 8.0 Hz, $^4J_{H,H}$ = 1.7 Hz, 1H; ***CH***-4), 7.09 (t, $^3J_{H,H}$ = 8.0 Hz, 1H; ***CH***-5), 5.15 (s, 2H; *m*-BnO ***CH***$_2$), 5.13 (s, 2H; *o*-BnO ***CH***$_2$), 3.86 ppm (s, 2H; ***CH***$_3$***O***); ^{13}C NMR (75 MHz, $CDCl_3$): δ = 166.8 (q; ***CO***$_2$***CH***$_3$), 152.8 (q; Ph ***C***-2), 148.3 (q; Ph ***C***-3), 137.4 (q; *o*-BnO ***C***-1), 136.6 (q; *m*-BnO ***C***-1), 128.5 (t; *o*/*m*-BnO ***CH***-3,5), 128.2 (t; *m*-BnO ***CH***-2,6), 128.0 (t; *o*-BnO ***CH***-4), 127.9 (t; *m*-BnO ***CH***-4), 127.5 (t; *o*-BnO ***CH***-2,6), 126.9 (q; Ph ***C***-1), 123.9 (t; Ph ***CH***-5), 122.9 (t; Ph ***CH***-6), 118.1 (t; Ph ***CH***-4), 75.6 (s; *o*-BnO ***CH***$_2$), 71.3 (s; *m*-BnO ***CH***$_2$), 52.1 ppm (p; ***CO***$_2$***CH***$_3$); IR (KBr): $\tilde{\nu}$ = 3064, 3032, 2949, 2880, 1730, 1580, 1489, 1474, 1433, 1374, 1263, 1147, 1083, 979, 916, 861, 783, 754, 697 cm^{-1}; UV/Vis (CH_2Cl_2): λ_{max} (ε) = 246 (3550), 294 nm (2630 mol^{-1} dm^3 cm^{-1}); FAB-MS: *m*/*z* (%): 348.3 (35) $[M]^+$, 371.3 (3) $[M+Na]^+$.

2,3-Bis(benzyloxy)benzoic acid (5b): Aqueous NaOH (2 M, 6.0 mL, 12.0 mmol) was added to a solution of **4** (2.090 g, 6.0 mmol) in MeOH (24 mL) and the mixture was stirred at 100 °C for 60 min. After the mixture had cooled down, water (100 mL) and HCl (2 M, 15 mL, 30.0 mmol) were added and the product was extracted with CH_2Cl_2 (3×50 mL). The organic layer was dried over $MgSO_4$, filtered and concentrated to give benzoic acid **5b** (1.943 g, 96.9 %) as a white powder. ^{1}H NMR (300 MHz, $CDCl_3$): δ = 7.65 (dd, $^3J_{H,H}$ = 7.8 Hz, $^4J_{H,H}$ = 1.5 Hz, 1H; Ph ***CH***-6), 7.42–7.28 (m, 5H; BnO ***CH***), 7.26 (s, 5H; BnO ***CH***), 7.18 (dd, $^3J_{H,H}$ = 7.8 Hz, $^4J_{H,H}$ = 1.5 Hz, 1H; Ph ***CH***-4), 7.10 (t, $^3J_{H,H}$ = 7.8 Hz, 1H; Ph ***CH***-5), 5.18 (s, 2H; *m*-BnO ***CH***$_2$), 5.11 ppm (s, 2H; *o*-BnO ***CH***$_2$); ^{13}C NMR (75 MHz, $CDCl_3$): δ = 165.3 (q; ***CO***$_2$***H***), 151.3 (q; Ph ***C***-2), 147.1 (q; Ph ***C***-3), 135.8 (q; *o*-BnO ***C***-1), 134.7 (q; *m*-BnO ***C***-1), 129.2 (t; *o*/*m*-BnO ***CH***-3,5), 128.79 (t; *m*-BnO ***CH***-2,6), 128.77 (t; *o*-BnO ***CH***-2,6), 128.5 (t; *o*-BnO ***CH***-4), 127.7 (t; *m*-BnO ***CH***-4), 125.0 (t; Ph ***CH***-5), 124.4 (t; Ph ***CH***-6), 123.1 (q; Ph ***C***-1), 119.0 (t; Ph ***CH***-4), 77.1 (s; *o*-BnO ***CH***$_2$), 71.5 ppm (s; *m*-BnO ***CH***$_2$); IR (KBr): $\tilde{\nu}$ = 3442, 3063, 3032, 2876, 2675, 2976, 1694, 1599, 1577, 1498, 1474, 1455, 1415, 1378, 1313, 1262, 1220, 1036, 967, 767, 752, 698 cm^{-1}; UV/Vis (CH_2Cl_2): λ_{max} (ε) = 246 (6310), 300 nm (4470 mol^{-1} dm^3 cm^{-1}); EI-MS: *m*/*z* (%): 334.2 (3) $[M]^+$, 243.1 (4), 225.1 (1), 181.2 (23), 91.1 (100), 65.2 (7).

2,3-Bis(benzyloxy)benzoyl chloride (6b): 2,3-Bis(benzyloxy)benzoic acid (0.669 g, 2.0 mmol) was stirred at reflux in thionyl chloride (10 mL) for three hours, and volatiles were then evaporated in vacuo to yield acid chloride **6b** (0.701 g, 99.4 %) as a yellowish oil. ^{1}H NMR (300 MHz, $CDCl_3$): δ = 7.61 (dd, $^3J_{H,H}$ = 8.0 Hz, $^4J_{H,H}$ = 1.5 Hz, 1H; Ph ***CH***-6), 7.49–7.34 (m, 10H; *o*/*m*-BnO ***CH***-2,3,4,5,6), 7.27 (dd, $^3J_{H,H}$ = 8.0 Hz, $^4J_{H,H}$ = 1.5 Hz, 1H; Ph ***CH***-4), 7.17 (t, $^3J_{H,H}$ = 8.0 Hz, 1H; Ph ***CH***-5), 5.19 (s, 2H; *m*-BnO ***CH***$_2$), 5.16 ppm (s, 2H, *o*-BnO ***CH***$_2$); ^{13}C NMR (75 MHz, $CDCl_3$): δ = 164.7 (q; ***COCl***), 152.7 (q; Ph ***C***-3), 148.0 (q; Ph ***C***-2), 136.5 (q; *m*-BnO ***C***-1), 136.0 (q; *o*-BnO, ***C***-1), 128.79 (t; *m*-BnO ***CH***-3,5), 128.65 (t; *o*-BnO ***CH***-3,5), 128.32 (t; *o*-BnO ***CH***-2,6), 128.26 (t; *o*-BnO ***CH***-4), 128.19 (t; *m*-BnO ***CH***-4), 127.5 (t; *m*-BnO ***CH***-2,6), 124.4 (t; Ph ***CH***-5), 124.0 (t; Ph ***CH***-6), 119.8 (t; Ph ***CH***-4), 75.7 (s; *o*-BnO ***CH***$_2$), 71.4 ppm (s; *m*-BnO ***CH***$_2$).

Methyl- and benzyl-protected precursors 8a and 8b: Hydrazine monohydrate (0.250 g, 5.0 mmol) was added to a solution of platform **7** (0.098 g, 0.10 mmol) in CH_2Cl_2/THF/EtOH 2:2:1 (25 mL), and stirring was continued at room temperature for 24 h. Volatiles were then removed in a rotary evaporator, and the residue was dried in vacuo (<1 mbar, 50 °C, 2 h). The remaining solid was suspended in CH_2Cl_2 (30 mL), followed by addition of the appropriate acid chloride (1.0 mmol) and triethylamine (0.152 g, 1.5 mmol). After the system had been stirred for 6 h at room temperature, the solvent was removed, and the residual solid was subjected to column chromatography (CH_2Cl_2/EtOAc/MeOH 75:25:0 → 75:25:5 for **8a**, EtOAc/MeOH 100:0 → 100:3 for **8b**) to provide the product.

Data for 8a: Yield: 0.099 g (99.2 %); TLC: R_f = 0.55 (CH_2Cl_2/EtOAc/MeOH 75:25:5; silica); ^{1}H NMR (500 MHz, $CDCl_3$): δ = 8.69 (t, $^3J_{H,H}$ = 6.0 Hz, 1H; ***CONHCH***$_2$), 8.17 (d, $^3J_{H,H}$ = 7.9 Hz, 1H, ***CONH***), 7.67 (dd, $^3J_{H,H}$ = 7.9 Hz, $^4J_{H,H}$ = 1.6 Hz, 1H; Ph ***CH***-6), 7.11 (t, $^3J_{H,H}$ = 7.9 Hz, 1H; Ph ***CH***-5), 7.02 (dd, $^3J_{H,H}$ = 7.9 Hz, $^4J_{H,H}$ = 1.6 Hz, 1H, Ph ***CH***-4), 5.087 (dd, $^2J_{H,H}$ = 15.8 Hz, $^3J_{H,H}$ = 6.3 Hz, 1H; ***CONHCH***$_2$), 5.087 (dd, $^3J_{H,H}$ = 7.9 Hz, $^3J_{H,H}$ = 4.7 Hz, 1H; Val α-***CH***), 4.94 (dd, $^2J_{H,H}$ = 15.8 Hz, $^3J_{H,H}$ = 6.3 Hz, 1H; ***CONHCH***$_2$), 3.86 (s, 6H; ***CH***$_3$***O***), 2.37–2.30 (m, 1H; Val β-***CH***), 1.04 (d, $^3J_{H,H}$ = 6.6 Hz, 3H; Val ***CH***$_3$), 1.01 ppm (d, $^3J_{H,H}$ = 6.6 Hz, 3H; Val ***CH***$_3$); ^{13}C NMR (125 MHz, $CDCl_3$): δ = 165.2 (q; ***CONHCH***$_2$), 161.5 (q; oxazole ***C***-2), 160.4 (q; ***CONH***), 153.2 (q; oxazole ***C***-5), 152.6 (q; Ph ***C***-3), 147.7 (q; Ph ***C***-2), 130.0 (q; oxazole ***C***-4), 126.0 (q; Ph ***C***-1), 124.2 (t; Ph ***CH***-5), 122.8 (t; Ph ***CH***-6), 115.7 (t; Ph ***CH***-4), 61.4 (p; ***CH***$_3$***O***-2), 56.0 (p; ***CH***$_3$***O***-3), 53.1 (p; Val α-***CH***), 34.2 (s; ***CONHCH***$_2$), 33.5 (t; Val β-***CH***), 18.4 (p; Val ***CH***$_3$), 18.2 ppm (p; Val ***CH***$_3$); UV/Vis (CH_2Cl_2): λ_{max} (ε) = 296 nm (8130 mol^{-1} dm^3 cm^{-1}); CD (CH_2Cl_2): λ ($\Delta\varepsilon$) = 250 nm (+8.6 mol^{-1} dm^3 cm^{-1}); ESI-HRMS: *m*/*z*: calcd for $[C_{54}H_{64}N_9O_{15}]^+$: 1078.4516; found: 1078.4561.

Data for 8b: Yield: 0.094 g (61.2 %). TLC: R_f = 0.68 (CH_2Cl_2/EtOAc/MeOH 75:25:3; silica); ^{1}H NMR (500 MHz, $CDCl_3$): δ = 8.55 (t, $^3J_{H,H}$ = 5.8 Hz, 1H; ***CONHCH***$_2$), 8.17 (d, $^3J_{H,H}$ = 7.8 Hz, 1H; ***CONH***), 7.71 (dd, $^3J_{H,H}$ = 5.7 Hz, $^4J_{H,H}$ = 3.9 Hz, 1H; Ph ***CH***-6), 7.44–7.41 (dd, $^3J_{H,H}$ = 8.0 Hz, $^4J_{H,H}$ = 1.5 Hz, 2H; *o*-BnO ***CH***-2,6), 7.39–7.33 (m, 3H; BnO ***CH***-3,4,5), 7.22–7.20 (dd, $^3J_{H,H}$ = 7.8 Hz, $^4J_{H,H}$ = 1.8 Hz, 2H; *m*-BnO ***CH***-2,6), 7.18–7.12 (m, 5H; BnO ***CH***-3,4,5, Ph ***CH***-4,5), 5.12 (s, 2H; *o*-BnO ***CH***$_2$), 5.08 (d, $^2J_{H,H}$ = 10.6 Hz, 1H; *m*-BnO ***CH***$_2$), 5.05 (d, $^2J_{H,H}$ = 10.6 Hz, 1H; *m*-BnO ***CH***$_2$), 5.01 (dd, $^2J_{H,H}$ = 15.9 Hz, $^3J_{H,H}$ = 6.3 Hz, 1H; ***CONHCH***$_2$), 4.99 (dd, $^3J_{H,H}$ = 7.8 Hz, $^3J_{H,H}$ = 4.6 Hz, 1H; Val α-***CH***), 4.86 (dd, $^2J_{H,H}$ = 15.9 Hz, $^3J_{H,H}$ = 5.4 Hz, 1H; ***CONHCH***$_2$), 2.32–2.26 (m, 1H; Val β-***CH***), 1.00 (d, $^3J_{H,H}$ = 6.8 Hz, 3H; Val ***CH***$_3$), 0.97 ppm (d, $^3J_{H,H}$ = 6.8 Hz, 3H; Val ***CH***$_3$); ^{13}C NMR (125 MHz, $CDCl_3$): δ = 165.1 (q; ***CONHCH***$_2$), 161.5 (q; oxazole ***C***-2), 160.1 (q; ***CONH***), 152.6 (q; oxazole ***C***-5), 151.7 (q; Ph ***C***-2), 146.7 (q; Ph ***C***-3), 136.3 (q; *o*-BnO ***C***-1), 136.0 (q; *m*-BnO ***C***-1), 129.8 (q; oxazole ***C***-4), 128.55 (t; BnO ***CH***), 128.51 (t; BnO ***CH***), 128.36 (t; BnO ***CH***), 128.13 (t; BnO ***CH***), 127.5 (t; BnO ***CH***), 126.9 (q; Ph ***C***-1), 124.3 (t; Ph ***CH***-5), 123.2 (t; Ph ***CH***-6), 117.3 (t; Ph ***CH***-4), 76.1 (s; *m*-BnO ***CH***$_2$), 71.2 (s; *o*-BnO ***CH***$_2$), 53.0 (t; Val α-***CH***), 34.1 (s; ***CONHCH***$_2$), 33.4 (t; Val β-***CH***$_3$), 18.3 (p; Val ***CH***$_3$), 18.1 ppm (p; Val ***CH***$_3$); UV/Vis (CH_2Cl_2): λ_{max} (ε) = 296 nm (8510 mol^{-1} dm^3 cm^{-1}); CD (CH_2Cl_2): λ ($\Delta\varepsilon$) = 250 nm (+10.1 mol^{-1} dm^3 cm^{-1}); ESI-HRMS: *m*/*z*: calcd for $[C_{90}H_{88}N_9O_{15}]^+$: 1535.6426; found: 1535.6483.

Ligand 1

Preparation from 8a: A BBr_3 solution (1 M in CH_2Cl_2, 0.70 mL, 0.70 mmol) was added to a solution of **8a** (0.054 g, 0.05 mmol) in CH_2Cl_2 (3 mL), and the mixture was stirred at room temperature for 16 h. MeOH was then added, and solvents were evaporated in vacuo. The residue was purified by column chromatography on silica gel (CH_2Cl_2/MeOH/HCO_2H 95:5:0.4) to give **1** (0.048 g, 96.4 %) as a grey solid.

Preparation from 8b: A solution of **8b** (0.031 g, 0.02 mmol) in MeOH (20 mL) was hydrogenated under atmospheric pressure for 6 h in the presence of Pearlman's catalyst (20 % $Pd(OH)_2$ on charcoal, 0.050 g). The catalyst was then filtered off, and the solvents were evaporated to give pure **1** (0.019 g, 95.7 %) as a white solid.

^{1}H NMR (500 MHz, [D$_4$]MeOH): δ = 7.16 (dd, $^3J_{H,H}$ = 8.0 Hz, $^4J_{H,H}$ = 1.4 Hz, 1H; Ph ***CH***-6), 6.89 (dd, $^3J_{H,H}$ = 8.0 Hz, $^4J_{H,H}$ = 1.4 Hz, 1H; Ph ***CH***-4), 6.66 (t, $^3J_{H,H}$ = 8.0 Hz, 1H; Ph ***CH***-5), 5.10 (d, $^3J_{H,H}$ = 4.8 Hz, 1H; Val α-***CH***), 4.88 (s, 2H; ***CONHCH***$_2$), 2.32–2.25 (m, 1H; Val β-***CH***), 0.99 (d, $^3J_{H,H}$ = 6.9 Hz, 3H; Val ***CH***$_3$), 0.92 ppm (d, $^3J_{H,H}$ = 6.9 Hz, 3H; Val ***CH***$_3$); ^{13}C NMR (125 MHz, [D$_4$]MeOH): δ = 171.5 (q; ***CONHCH***$_2$), 162.8

(q; oxazole ***C***-2), 162.0 (q; ***CONH***), 154.2 (q; oxazole ***C***-5), 150.4 (q; Ph ***C***-2), 147.4 (q; Ph ***C***-3), 130.8 (q; oxazole ***C***-4), 119.9 (t; Ph ***CH***-4), 119.7 (t; Ph ***CH***-5), 118.8 (t; Ph ***CH***-6), 116.3 (q; Ph ***C***-1), 54.5 (t; Val α-***CH***), 35.4 (s; *CONH**CH**$_2$*), 34.7 (t; Val β-***CH**$_3$*), 18.7 (p; Val ***CH**$_3$*), 18.5 ppm (p; Val ***CH**$_3$*); ESI-HRMS: *m*/*z*: calcd for $[C_{48}H_{52}N_9O_{15}]^+$: 994.3577; found: 994.3521.

UV absorption and CD spectrophotometric titrations: For the UV absorption and CD spectrophotometric titrations, titrant solution containing only **1** ($[\mathbf{1}]=2.0\times10^{-5}$ M in MeOH/H_2O 10:90; tris/HCl buffer 0.10 M/0.02 M at pH 8.95) and titrant solution containing both **1** and the appropriate metal salt ($[\mathbf{1}]=2.0\times10^{-5}$ M, $[M^{n+}]=3.0\times10^{-4}$–$5.0\times10^{-4}$ M in MeOH/H_2O 10:90 in tris/HCl buffer 0.10 M/0.02 M at pH 8.95) were prepared. Titrant solution (2500 μL) was placed in the 1 cm-pathlength quartz cuvette containing a stirring magnet. Automatized titrations were performed at 20 °C by addition of titrant solution in discrete steps (10 μL) and recording of spectra after a suitable mixing time (3–15 min).

A manual titration experiment for Job plot analysis was performed with ligand and metal salt solutions of the same concentration (3.0×10^{-5} M in MeOH/H_2O 10:90; tris/HCl buffer 0.10 M/0.02 M at pH 8.95). Ligand solution (2500 μL) was placed in the cuvette, and spectra were measured. In each titration step an aliquot (100 → 1000 μL) was removed from the cuvette and the same volume of metal salt solution was added. After sufficient equilibrating time, spectra were measured. Finally, spectra from the pure metal salt solution were taken.

Acknowledgement

This work was generously supported by the Deutsche Forschungsgemeinschaft. The authors thank Dr. Andreea Schuster for helpful discussions.

[1] a) I. G. O'Brien, F. Gibson, *Biochim. Biophys. Acta* **1970**, *215*, 393–402; b) J. R. Pollack, J. B. Neilands, *Biochem. Biophys. Res. Commun.* **1970**, *38*, 989–992.
[2] L. D. Loomis, K. N. Raymond, *Inorg. Chem.* **1991**, *30*, 906–911.
[3] S. S. Isied, G. Kuo, K. N. Raymond, *J. Am. Chem. Soc.* **1976**, *98*, 1763–1767.
[4] a) D. J. Ecker, L. D. Loomis, M. E. Cass, K. N. Raymond, *J. Am. Chem. Soc.* **1988**, *110*, 2457–2464; b) T. B. Karpishin, T. D. P. Stack, K. N. Raymond, *J. Am. Chem. Soc.* **1993**, *115*, 6115–6125.
[5] L. D. Loomis, K. N. Raymond, *Inorg. Chem.* **1991**, *30*, 906–911.
[6] D. S. Plaha, H. J. Rogers, *Biochim. Biophys. Acta* **1983**, *760*, 246–255.
[7] J. V. McArdle, S. R. Sofen, S. R. Cooper, K. N. Raymond, *Inorg. Chem.* **1978**, *17*, 3075–3078.
[8] a) T. B. Karpishin, T. M. Dewey, K. N. Raymond, *J. Am. Chem. Soc.* **1993**, *115*, 1842–1851; b) T. B. Karpishin, K. N. Raymond, *Angew. Chem.* **1992**, *104*, 486–488; *Angew. Chem. Int. Ed. Engl.* **1992**, *31*, 466–468.
[9] R. C. Hider, J. Silver, J. B. Neilands, I. E. G. Morrison, L. V. C. Rees, *FEBS Lett.* **1979**, *102*, 325–328.
[10] J. B. Neilands, T. J. Erickson, W. H. Rastetter, *J. Biol. Chem.* **1981**, *256*, 3831–3832.
[11] K. N. Raymond, G. Müller, B. F. Matzanke, *Top. Curr. Chem.* **1984**, *123*, 49–102.
[12] a) A. Shanzer, J. Libman, S. Lifson, C. E. Felder, *J. Am. Chem. Soc.* **1986**, *108*, 7609–7619; b) B. P. Hay, D. A. Dixon, R. Vargas, J. Garza, K. N. Raymond, *Inorg. Chem.* **2001**, *40*, 3922–3935.
[13] E. J. Corey, S. D. Hurt, *Tetrahedron Lett.* **1977**, *18*, 3923–3924.
[14] a) M. Lofthagen, R. VernonClark, K. K. Baldridge, J. S. Siegel, *J. Org. Chem.* **1992**, *57*, 61–69; b) M. Lofthagen, J. S. Siegel, M. Hackett, *Tetrahedron* **1995**, *51*, 6195–6208.
[15] A. W. Coleman, C. C. Lin, M. Miocque, *Angew. Chem.* **1992**, *104*, 1402–1404; *Angew. Chem. Int. Ed. Engl.* **1992**, *31*, 1381–1383.
[16] B. Tse, Y. Kishi, *J. Org. Chem.* **1994**, *59*, 7807–7814.
[17] For some examples of C_3-symmetric catecholate complexes see: a) M. D. Pluth, R. G. Bergman, K. N. Raymond, *J. Am. Chem. Soc.* **2007**, *129*, 11459–11467; b) I. Janser, M. Albrecht, K. Hunger, S. Burk, K. Rissanen, *Eur. J. Inorg. Chem.* **2006**, 244–251; c) W. Cai, S. W. Kwok, J. P. Taulane, M. Goodman, *J. Am. Chem. Soc.* **2004**, *126*, 15030–15031; d) M. Albrecht, I. Janser, J. Runsink, G. Raabe, P. Weis, R. Fröhlich, *Angew. Chem.* **2004**, *116*, 6832–6836; *Angew. Chem. Int. Ed.* **2004**, *43*, 6662–6666; e) M. Meyer, B. Kersting, R. E. Powers, K. N. Raymond, *Inorg. Chem.* **1997**, *36*, 5179–5191; f) M. Albrecht, R. Fröhlich, *J. Am. Chem. Soc.* **1997**, *119*, 1656–1661; g) B. Kersting, M. Meyer, R. E. Powers, K. N. Raymond, *J. Am. Chem. Soc.* **1996**, *118*, 7221–7222.
[18] B. Tse, Y. Kishi, *J. Am. Chem. Soc.* **1993**, *115*, 7892–7893.
[19] a) Y. Tor, J. Libman, A. Shanzer, S. Lifson, *J. Am. Chem. Soc.* **1987**, *109*, 6517–6518; b) Y. Tor, J. Libman, A. Shanzer, C. E. Felder, S. Lifson, *J. Am. Chem. Soc.* **1992**, *114*, 6661–6671.
[20] G. Haberhauer, *Angew. Chem.* **2007**, *119*, 4476–4479; *Angew. Chem. Int. Ed.* **2007**, *46*, 4397–4399.
[21] G. Haberhauer, *Angew. Chem.* **2008**, *120*, 3691–3694; *Angew. Chem. Int. Ed.* **2008**, *47*, 3635–3638.
[22] G. Haberhauer, T. Oeser, F. Rominger, *Chem. Commun.* **2005**, 2799–2801.
[23] Á. Pintér, G. Haberhauer, *Eur. J. Org. Chem.* **2008**, 2375–2387.
[24] Synthesis of acid chloride **6a**: M. E. Jung, S. Abrecht, *J. Org. Chem.* **1988**, *53*, 423–425; synthesis of acid chloride **6b**: a) S. K. Sharma, M. J. Miller, S. M. Payne, *J. Med. Chem.* **1989**, *32*, 357–367; b) R. A. Gardner, R. Kinkade, C. Wang, O. Phanstiel, *J. Org. Chem.* **2004**, *69*, 3530–3537.
[25] D. N. Caulder, C. Brückner, R. E. Powers, S. König, T. N. Parac, J. A. Leary, K. N. Raymond, *J. Am. Chem. Soc.* **2001**, *123*, 8923–8938.
[26] C.-F. Chow, M. H. W. Lam, W-Y. Wong, *Inorg. Chem.* **2004**, *43*, 8387–8393.
[27] a) R. D. Shannon, C. T. Prewitt, *Acta Crystallogr. Sect. B* **1969**, *25*, 925–946; b) R. D. Shannon, *Acta Crystallogr. Sect. A* **1976**, *32*, 751–767.
[28] a) S. Salama, J. D. Stong, J. B. Neilands, T. G. Spiro, *Biochemistry* **1978**, *17*, 3781–3785; b) M. E. Bluhm, S. S. Kim, E. A. Dertz, K. N. Raymond, *J. Am. Chem. Soc.* **2002**, *124*, 2436–2437.
[29] All computations were performed with the Gaussian 03 program-package: Gaussian 03, Revision C.02, M. J. Frisch, G. W. Trucks, H. B. Schlegel, G. E. Scuseria, M. A. Robb, J. R. Cheeseman, J. A. Montgomery, Jr., T. Vreven, K. N. Kudin, J. C. Burant, J. M. Millam, S. S. Iyengar, J. Tomasi, V. Barone, B. Mennucci, M. Cossi, G. Scalmani, N. Rega, G. A. Petersson, H. Nakatsuji, M. Hada, M. Ehara, K. Toyota, R. Fukuda, J. Hasegawa, M. Ishida, T. Nakajima, Y. Honda, O. Kitao, H. Nakai, M. Klene, X. Li, J. E. Knox, H. P. Hratchian, J. B. Cross, V. Bakken, C. Adamo, J. Jaramillo, R. Gomperts, R. E. Stratmann, O. Yazyev, A. J. Austin, R. Cammi, C. Pomelli, J. W. Ochterski, P. Y. Ayala, K. Morokuma, G. A. Voth, P. Salvador, J. J. Dannenberg, V. G. Zakrzewski, S. Dapprich, A. D. Daniels, M. C. Strain, O. Farkas, D. K. Malick, A. D. Rabuck, K. Raghavachari, J. B. Foresman, J. V. Ortiz, Q. Cui, A. G. Baboul, S. Clifford, J. Cioslowski, B. B. Stefanov, G. Liu, A. Liashenko, P. Piskorz, I. Komaromi, R. L. Martin, D. J. Fox, T. Keith, M. A. Al-Laham, C. Y. Peng, A. Nanayakkara, M. Challacombe, P. M. W. Gill, B. Johnson, W. Chen, M. W. Wong, C. Gonzalez, J. A. Pople, Gaussian, Inc., Wallingford CT, **2004**.
[30] M. Karplus, *J. Am. Chem. Soc.* **1963**, *85*, 2870–2871.
[31] G. Haberhauer, E. Drosdow, T. Oeser, F. Rominger, *Tetrahedron* **2008**, *64*, 1853–1859.

Received: July 30, 2008
Revised: September 12, 2008
Published online: November 6, 2008

